### Current Research in

## Chemistry



Current Research in Chemistry 4 (3): 60-67, 2012 ISSN 1996-5052 / DOI: 10.3923/crc.2012.60.67 © 2012 Knowledgia Review, Malaysia

# Synthesis and Characterization of Nano Crystalline Tin(IV) Oxide from Tin(II) Chloride Using Combined Microwave and Traditional Calcinations Procedures

<sup>1</sup>Sudha Parimala, <sup>2</sup>S. Christina Selin, <sup>2</sup>A. Gnanamani and <sup>1</sup>A.B. Mandal

<sup>1</sup>Chemical Laboratory, <sup>2</sup>Microbiology Division, Central Leather Research Institute (CSIR, New Delhi), Chennai, India

Corresponding Author: A.B. Mandal, Director, Central Leather Research Institute (CSIR, New Delhi), Adyar, Chennai 20, Tamil Nadu, India

#### ABSTRACT

Today, simple, cost effective and efficient methods are needed to prepare promising nano sized metal oxides. The aim of our study was to prepare nano crystalline tin oxide with higher surface area and less agglomeration from a cheaper precursor with modification of the reported methodologies followed by its characterisation. Tin oxide was synthesised from tin(II) chloride by sol-gel method followed by the combined microwave pre calcinations for five minutes and traditional calcinations at 400°C for 2 h. The X ray diffraction patterns of the calcined product showed the formation of high purity tetragonal tin(IV) oxide with the crystallite size in the range of 14 to 16 nm as calculated by Sherer method. The lattice strain was calculated by Williamson-Hall method and found to be 0.33 percent. The lattice parameters were also calculated. The crystalline product also showed good morphology with meagre agglomeration as illustrated by TEM micrographs. Ultimately the study provided a viable and energy efficient synthetic route for nanocrystalline tin(IV) oxide which finds immense applications.

**Key words:** Nano crystalline, tin(IV) oxide, tin(II) chloride, precalcinations, XRD, TEM

#### INTRODUCTION

Metals and Metal oxides of nano size displayed wide ranging applications from semiconductor to targeted drug delivery systems. Amongst the various metal oxides, tin oxide show promising applications. Research on tin oxide attracts a lot due to its wide range of applications as gas sensors for gases like CO, hydrocarbons, ammonia, hydrogen, heat mirrors, and transparent electrodes for solar cells, opto-electronic devices and as catalysts (Bhagwat et al., 2003). The presence of surface oxygen species on tin(IV) oxide greatly influences its sensing and catalytic properties which in turn are related to the heat treatment during its preparation (Harrison and Willett, 1988). Recently, it has been studied as overcoat for thin film magnetic recording media (Novotny and Kao, 1990), as transparent electrode in panels and other electro chromic devices, and also in photo electrochemical studies and those related to the development of solar cells (Nasr et al., 1998). It is also investigated as a material for Li-ion batteries (Liu et al., 1998; Retoux et al., 1999). In addition, its relative cheaper cost widens its applications in all walks of human life compared to other available materials of similar functions. Recently, more research focus has been given to increase the sensitivity, selectivity and stability of tin oxide. SnO<sub>2</sub> is an n-type semiconductor with wide band gap energy

(3.6 eV) due to the presence of oxygen vacancies, which electronically act as electron donors. Fajardo *et al.* (2008) showed SnO<sub>2</sub>nano particles as active catalysts for the ethanol steam reforming reaction and correlated the catalytic selectivity of nano tin oxide with its doping and annealing temperatures.

Baneto et al. (2010) synthesized ZnO film doped with Sn by Spray Pyrolysis and Chemical Deposition methods and found a difference in the dependence of morphology of the film on tin content in both the methods. In the spray pyrolysis method, Sn(II) chloride is used as the precursor and the product obtained is crystalline with a crystallite size of more than 100 nm. Also, nanorods with pyramidal shape which are not well faceted were obtained. Ramli and Abu Bakar (2011) prepared tin doped with alumina by the incipient impregnation method followed by calcinations in a domestic microwave oven and such synthesized material is used as a catalyst for the degradation of polystyrene. In their process tin(IV) chloride is used as a precursor and calcinations are done by using domestic microwave oven and traditional heating for a period of 5 min and 16 h, respectively and the microwave heated product showed better surface area and hence better catalytic activity. According to Ristic et al. (2002), all the characteristic properties of SnO<sub>2</sub> depend on the crystallite size and specific surface area of which in turn depends on the nature of the calcinations process.

In general, the nature of microstructured/nanostructured materials depends on the method of preparation. With regard to  $\mathrm{SnO_2}$  nanoparticles, methods such as, hydrothermal (Mori et al., 2002), Solvothermal (Deng et al., 2002), Sol-gel (Kakihana, 1996; Broussous et al., 2002), and amorphous citrate route (Bhagwat et al., 2003) are being followed to get well defined crystallites However, sol-gel process is more widely followed and accepted because of the versatility and the ease of fabrication of nanoparticles (Zhang and Gao, 2004). In this process metal oxides or their salts act as precursors which can undergo simple chemical reactions like hydrolysis or condensation reactions to form a network of dispersions or colloidal solution which consist of amorphous or submicron sized particles dispersed in various directions in the host system. Sedimentation, washing and calcinations are the sequential processes followed in the preparation. The resulting product can be calcined at various temperatures and time durations. In order to reduce the thermal energy and time consumed for the said process, alternate methods are in need of the hour. We have to keep in mind that the chosen alternate procedures should not affect the quality and the properties of  $\mathrm{SnO}_{\circ}$ .

In the present study Sn(II) chloride was used as a precursor which was very easy to handle and cost effective for the preparation of Sn(IV) oxide through the sol-gel process. Previous reports indicate that calcinations at higher temperatures lead to a significant decline in surface area which may be due to severe aggregation of the  $SnO_2$  nanoparticles. The present study explored the possibility of reducing the time taken for the calcinations and agglomeration of the nanoparticles. This was done by pre heating the prepared gel using microwave and traditional calcinations. XRD and TEM analysis were used for the characterisation of the synthesised sample.

#### MATERIALS AND METHODS

**Chemicals required:** The chemicals used in the present study were tin(II) chloride dihydrate (SnCl<sub>2</sub>.2H<sub>2</sub>O, Qualigens), Ammonium hydroxide (NH<sub>4</sub>OH 25%), Ethanol (C<sub>2</sub>H<sub>5</sub>OH, 99.9% Absolute alcohol, Merck, Bombay). All reagents were used as received without any further purification.

**Preparation:** About 3.0 g of tin(II) chloride was added to 50 mL water in a round bottom flask and was stirred for 20 min. About 4 mL of ammonia solution (25%) was added under a controlled feed rate at 0.1 mL min<sup>-1</sup> with constant stirring. The pH values were maintained in the range between 1 to 10.2 and reaction the temperature 70°C. After 2 h of stirring, the sol was aged at room

temperature for 24 h. The pH of the resulting gel was kept as neutral after washing with ethanol. Then the gel was pre-calcined by microwave radiation (using domestic microwave oven) for 5 min at 100 watts with the time interval of 1 min. The powder obtained from the above step was ground using mortar and pestle and finally calcined at 400°C for 2 h in muffle furnace. The sample thus obtained was characterized in the following way.

Instrumental analyses: The bulk property of SnO<sub>2</sub> obtained from the above step was studied by FT-IR, XRD and the surface morphology was studied by TEM. FT-IR spectra were recorded using a FT-IR model Shimadzu spectrometer. The spectra were collected from 4000 to 400 cm<sup>-1</sup>. All spectra were recorded against the background spectra of KBr. The morphology and dimension of the sample was taken on a JEOL model-200cx using an accelerating voltage of 120 kV. Samples for the TEM were prepared by ultrasonically dispersing the sample in ethanol, and then droplets were placed on carbon coated Cu grids.

X-ray diffraction analysis: The crystalline phases of the sample were identified by X-ray diffraction (XRD) using a Regaku cd-max 2 vc model, using a Cu-Kα radiation filtered by nickel foil over the range of 2-80° (20). Crystallite sizes (D) were calculated using Scherrer's equation:

$$D = k\lambda/\beta \cos\theta$$

where, k is the shape factor  $\lambda$  is the X-ray wavelength.  $\beta$  is the line broadening at half the maximum intensity (FWHM) in radians and  $\theta$  is the Bragg angle. D is the mean size of the ordered domains which may be smaller or equal to the grain size. The dimensionless shape factor has a typical value of about 0.9 which varies with the actual shape of the crystallite. The Scherrer equation is limited to nano scale particles. It is not applicable to grains larger than about 0.1  $\mu$ m which precludes those observed in most metallographic and ceramographic microstructures. It is important to realize that the Scherrer formula provides a lower bound on the particle size. A variety of factors (particle size, inhomogeneous strain and instrumental errors) can contribute to the width of a diffraction peak. If the contributions of all these factors are zero, then the peak width would be determined solely for the particle size using Scherrer formula.

Generally, the broadening of the diffraction peaks depends upon two predominant factors; strain and particle size. We wanted to study the contribution of lattice strain towards the peak broadening. The strain if any can be calculated using Williamson and Hall theorem as shown below:

$$\beta \cos\theta/\lambda = 1/D + \eta \sin\theta/\lambda$$

where,  $\beta$  is the full width at half-maximum (FWHM),  $\theta$  is the diffraction angle,  $\lambda$  is the X-ray wavelength, D is the effective particle size and  $\eta$  is the effective strain. In our study the strain and crystallite size were measured from the slope and intercept of the plot of  $\beta \cos\theta/\lambda$  against  $\sin\theta/\lambda$ .

#### RESULTS AND DISCUSSION

The sample obtained after calcinations was collected and found to be fine powder, half white in colour, insoluble in water but sparingly soluble in methanol and completely soluble in aqua regia. Figure 1a and b displayed the FT-IR spectra of the sample received during pre-calcination and after complete calcinations respectively. Spectra of pre-calcined samples displayed

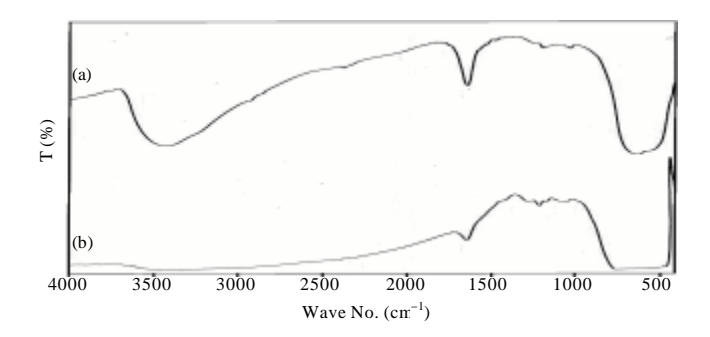


Fig. 1(a-b): (a) FT-IR Spectrum of  $SnO_2$  nanoparticles after microwave exposure for 5 min, (b) FT-IR spectrum of  $SnO_2$  nanoparticles after complete calcination at  $400^{\circ}$ C for 2 h

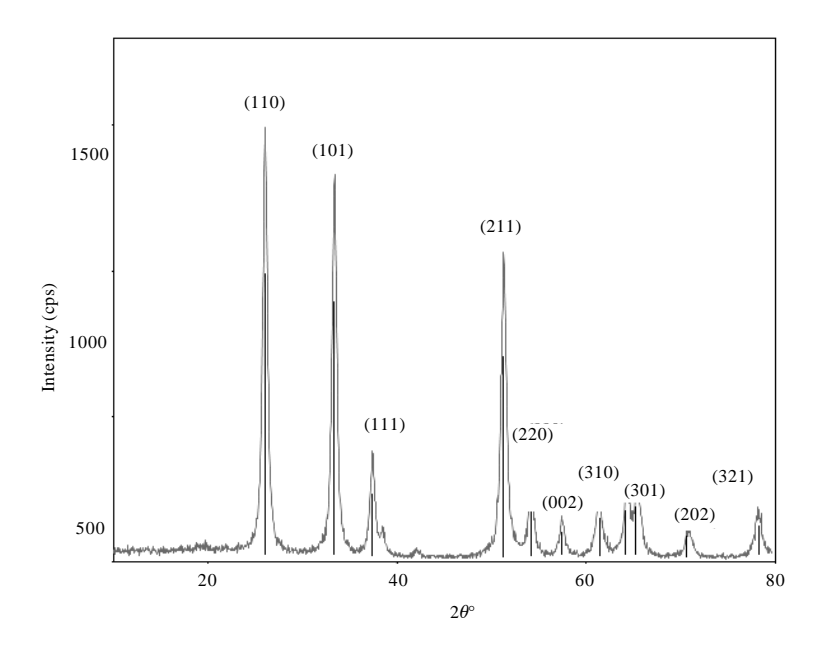


Fig. 2: XRD pattern of SnO<sub>2</sub> nanoparticles obtained from tin(II) chloride using combined microwave and traditional calcination methods

broad peak at 3400 cm<sup>-1</sup> corresponding to -OH stretch, a small hump at 2950 and 1630 cm<sup>-1</sup> which corresponds to -C-H- stretch of the impurities present. However, after calcinations, the sample displayed no intense broad peak at 3400 cm<sup>-1</sup> and the peak at 2950 cm<sup>-1</sup> disappeared, peak at 1631 cm<sup>-1</sup> reduced indicating the completion of calcinations. The absorption peaks near 550 and 650 cm<sup>-1</sup> corresponds to Sn-O and O-Sn-O vibrations, respectively. The characteristic peaks in the regions of 625-665 and 1040-1060 cm<sup>-1</sup> corresponds to O-Sn-O- bridge of the functional group of SnO<sub>2</sub>. The band at 1040-1060 cm<sup>-1</sup>, characteristics of Sn = O and Sn-O bands, indicates the presence of adsorbed oxygen species intermediate between  $O_2^-$  and  $O_2^{2-}$  (Gundrizer and Davydov, 1975). The number of small peaks in the range between 400-555 cm<sup>-1</sup> displayed by the sample imply the higher conversion of Sn to SnO<sub>2</sub> (Davydov and Sheppard, 2003; Zhang and Gao, 2004).

Figure 2 demonstrated XRD patterns of the sample. Intense peaks at  $2\theta$  values of 26.3, 33.6, 37.8, 38.7, 51.5, 54.5, 57.5, 61.7, 64.5, 65.7, 70.9, 78.5 (values in A°) observed matches with the

Table 1: Comparison on d-values of JCPDS and the calculated d-values of  $SnO_2$  obtained from the combined microwave and traditional calcination method

Standard d values (JCPDS 21-1250)	Obtained d value	Planes
3.350	3.372	110
2.644	2.652	101
2.369	2.380	200
1.765	1.768	211
1.678	1.682	220
1.593	1.594	002
1.498	1.500	310
1.439	1.442	112
1.415	1.4221	301

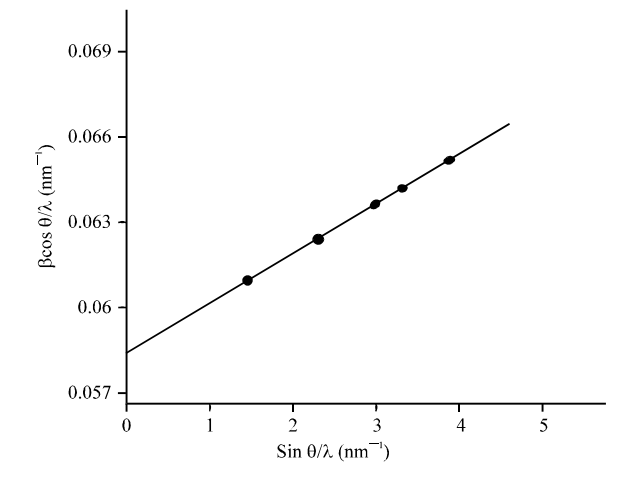


Fig. 3: Correlation between  $\beta\cos\theta/\lambda$  against  $\sin\theta/\lambda$  calculated from XRD analysis

patterns of bulk  $\mathrm{SnO_2}$  (ICDD 211250). The peak position and the relative intensity clearly confirmed the presence of highly crystalline single tetragonal rutile phase of  $\mathrm{SnO_2}$ . Furthermore, the crystallite (or crystal) size of each sample for all the prominent planes (110,101,200,211,220,310,301) was calculated using Scherrer formula using X ray wavelength of 1.5406 A. Accordingly, the average crystallite size in the prominent planes was found to be 14 nm. The broadening of the peaks further indicated that the particles were nano in size. The d values of the sample was compared with the d values of standard  $\mathrm{SnO_2}$  summarized by JCPDS 21-1250 and found the  $\Delta d$  was <1% (Table 1).

In addition, X-Ray diffraction analysis using XRDA program with quadratic smoothening of the curve and Lorentzian peak fitting suggested that all the diffraction peaks were readily indexed to the tetragonal phase of cassiterite  $\mathrm{SnO}_2$  with calculated lattice parameters a = 4.7428±0.0058, c = 3.1988±0.0089, da = 0.6745±0.0019 and V = 71.954 A. The results also indicated the high crystallinity of the prepared  $\mathrm{SnO}_2$  nanoparticles.

Figure 3 demonstrated the plot of  $\beta\cos\theta/\lambda$  against  $\sin\theta/\lambda$  for the prepared  $SnO_2$  nanoparticle. The plot showed a positive slope of 0.0033, suggesting the presence of tensile strain of 0.33% and a intercept which gave the crystallite size as 16.87 nm that was in good agreement with the value of 14.56 nm calculated from Scherrer's equation.

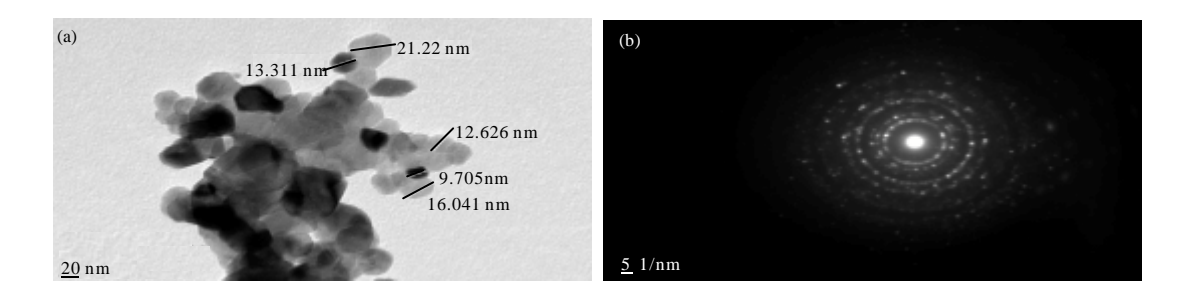


Fig. 4(a-b): (a) TEM images of SnO<sub>2</sub> nanoparticles obtained from tin(II) chloride, (b) Debye rings of SnO<sub>2</sub> nanoparticles obtains from tin(II) chloride

As: Particle size calculated from Scherrer equation = 14.56 nm Particle size calculated from Williamson and Hall equation = 16.87 nm Effective strain = +0.33%

In the year 2001, Morazzoni et al. (2001) prepared the nanostructured thin films of  $SnO_2$  (size 80 nm) and Pt-doped  $SnO_2$  by a new sol-gel route using tetra (tert-butoxy) tin(IV) and bis (acetylacetonato) platinum(II) as metal precursors. Adnan et al. (2010) prepared  $SnO_2$  nanoparticles using tin(IV) chloride by simple conventional sol-gel technique and obtained particles size in the range of 4 to 5.6 nm. Kar et al. (2011) obtained the crystallite size in the range of 2-3 nm using microwave irradiation method for calcinations. In the present study the advantage of both the methods were considered to get better results.

The TEM morphologies along with a typical Selected Area Electron Diffraction (SAED) pattern of the synthesized powder showed the nano range of the granular particles (Fig. 4a and b). It can be shown that the powder consisted of faceted grain structure (square like). A corresponding SAED pattern revealed the different Debye rings of  $\mathrm{SnO_2}$  as analyzed by XRD (Fig. 4b). From the dark contrast in the SAED pattern, the crystallites which were close to the Bragg orientations were identified with interplanar spacings assigned to the rutile structure. Also the grain size distribution was smaller with mean grain size of 15 nm. It may be concluded that the microwave pre calcined powders were less agglomerated as reported by Srivastava et al. (2006). According to Yoo et al. (1996), a wet process like sol-gel method give rather spherical grains but the TEM images of the sample of our study clearly indicated the formation of closed grains.

#### CONCLUSION

The novelty of the present study lies with the preparation of nanocrystalline tin oxide from tin(II) chloride as the precursor and the use of microwave heating for precalcination for a shorter period of time. This step ultimately reduced the time and thermal energy consumption during the calcinations for the preparation of nanoparticles of  $SnO_2$  which was for a period of two hours. The resulting product was crystalline with less agglomeration and hence more surface area. Also, the process used the economically lower cost chemical, tin(II) chloride as the precursor. Further study of bulk and surface property of the synthesized nano crystalline tin(IV) oxide using Raman spectra, BET isotherms and X ray photoelectron spectra will give additional information about the suitability of the product for wider applications as discussed before.

#### ACKNOWLEDGEMENTS

The author S. Sudhaparimala is thankful to the University Grants Commission, New Delhi for the award of Fellowship under UGC-FIP XI Plan and also to IIT, Madras for providing the TEM facility.

#### REFERENCES

- Adnan, R., N.A. Razana, I.A. Rahaman and M.A. Farrukh, 2010. Synthesis and characterization of high surface area tin oxide nanoparticles via the Sol-gel method as a catalyst for the hydrogenation of styrene. J. Chinese Chem. Soc., 57: 222-229.
- Baneto, M., Y. Lare, L. Cattin, M. Addou and K. Jondo *et al.*, 2010. Comparison of the structural and morphological properties of Sn doped ZnO films deposited by spray pyrolysis and chemical bath deposition. Asian J. Mater. Sci., 2: 196-203.
- Bhagwat, M., P. Shah and V. Ramaswamy, 2003. Synthesis of nanocrystalline SnO<sub>2</sub> powder by amorphous citrate route. Mater. Lett., 57: 1604-1611.
- Broussous, L., C.V. Santilli, S.H. Pulcinelli and A.F. Craievich, 2002. SAXS study of formation and growth of tin oxide nanoparticles in the presence of complexing ligands. J. Phys. Chem. B., 106: 2855-2860.
- Davydov, A.A. and N. Sheppard, 2003. Molecular Spectroscopy of Oxide Catalyst Surfaces. John Wiley and Sons, England, pp: 44-52.
- Deng, Z.X., C. Wang and Y.D. Li, 2002. New hydrolytic process for producing zirconium dioxide, tin dioxide and titanium dioxide nanoparticles. J. Am. Ceram. Soc., 85: 2837-2839.
- Fajardo, H.V., E. Longo, L.F.D. Probst, A. Valentini and N.V. Carreno *et al.*, 2008. Influence of rare earth doping on the structural and catalytic properties of nanostructured tin oxide. Nanoscale Res. Lett., 3: 194-199.
- Gundrizer, T.A. and A.A. Davydov, 1975. Infrared spectra of oxygen adsorbed on O2, Reac. Kinet. Catal. Lett., 3: 67-70.
- Harrison, P.G. and M.J. Willett, 1988. The mechanism of operation of tin(iv) oxide carbon monoxide sensors. Nature, 332: 337-339.
- Kakihana, M., 1996. Preparation of high temperature superconducting oxides. J. Sol-Gel Sci. Technol., 6: 7-55.
- Kar, A., S. Kundu and A. Patra, 2011. Surface defect-related luminescence properties of SnO<sub>2</sub> nanorods and nanoparticles. J. Phy. Chem., 115: 118-124.
- Liu, W., X. Huang, Z. Wang, H. Li and L. Chen, 1998. Study of stannic oxide as an anode material for lithium-ion batteries. J. Electrochem. Soc., 145: 59-62.
- Morazzoni, F., C. Canevali, N. Chiodini, C. Mari and R. Ruffo *et al.*, 2001. Nanostructured pt-doped tin oxide films:?Sol-gel preparation, spectroscopic and electrical characterization. Chem. Mater., 13: 4355-436.
- Mori, T., S. Hoshino, A. Neramittagapon, J. Kubo and Y. Morikawa, 2002. Novel activity of SnO<sub>2</sub> for methanol conversion: Formation of methane, carbon dioxide and hydrogen. Chem. Lett., 29: 390-391.
- Nasr, C., P.V. Kamat and S. Hotchandani, 1998. Photoelectrochemistry of composite semiconductor thin films. II. Photosensitization of SnO<sub>2</sub>/TiO<sub>2</sub> coupled system with a ruthenium polypyridyl complex. J. Phys. Chem. B., 102: 10047-10056.
- Novotny, V.J. and A.S. Kao, 1990. Tin oxide overcoats for thin film magnetic recording media. IEEE Trans. Magnet., 26: 2499-2501.

#### Curr. Res. Chem., 4 (3): 60-67, 2012

- Ramli, A. and D.R. Abu Bakar, 2011. Effect of calcination method on the catalytic degradation of polystyrene using Al<sub>2</sub>O<sub>3</sub> supported Sn and Cd catalysts. J. Applied Sci., 11: 1346-1350.
- Retoux, R., T. Brousse and D.M. Schleich, 1999. High-resolution electron microscopy investigation of capacity fade in SnO2 electrodes for lithium-ion batteries. J. Electrochem. Soc., 146: 2472-2476.
- Ristic, M., M. Ivanda, S. Popovic and S. Music, 2002. Dependence of nanocrystalline SnO2 particle size on synthesis route. J. Non-Crystal Solids., 303: 270-280.
- Srivastava, A., K.J. Rashmi, A.K. Srivastava and S.T. Lakshmikumar, 2006. Study of structural and microstructural properties of SnO2 powder for LPG and CNG gas sensors mater. Chem. Phy., 97: 85-90.
- Yoo, D.J., J. Tamaki, S.J. Park, N. Miiura and N. Yamazoe, 1996. Suppression of grain growth in sol-gel derived tin dioxide ultra thin films. J. Am. Ceram. Soc., 79: 2201-2204.
- Zhang, J. and L. Gao, 2004. Synthesis and characterization of nanocrystalline tin oxide by sol-gel method. J. Solid State Chem., 177: 1425-1430.